HHS Public Access

Author manuscript

Clin Cancer Res. Author manuscript; available in PMC 2021 July 19.

Published in final edited form as:

Clin Cancer Res. 2021 February 15; 27(4): 1139–1149. doi:10.1158/1078-0432.CCR-20-3139.

Cobomarsen, an Oligonucleotide Inhibitor of miR-155, Slows DLBCL Tumor Cell Growth *In Vitro* and *In Vivo*

Eleni Anastasiadou[1,2], **Anita G. Seto**[3], **Xuan Beatty**[3], **Melanie Hermreck**[3], **Maud-Emmanuelle Gilles**[1], **Dina Stroopinsky**[4], **Lauren C. Pinter-Brown**[5], **Linda Pestano**[3], **Cinzia Marchese**[2], **David Avigan**[4], **Pankaj Trivedi**[2], **Diana M. Escolar**[3], **Aimee L. Jackson**[3], **Frank J. Slack**[1]

[1]HMS Initiative for RNA Medicine, Department of Pathology, Beth Israel Deaconess Medical Center, Harvard Medical School, Boston, Massachusetts.

[2]Department of Experimental Medicine, Sapienza University of Rome, Italy.

[3]miRagen Therapeutics, Inc, Boulder, Colorado.

[4]Department of Hematology, Beth Israel Deaconess Medical Center, Harvard Medical School, Boston, Massachusetts.

[5]Department of Internal Medicine, Division of Hematology/Oncology, University of California, Irvine, California.

Abstract

Purpose: miRNA-155 is an oncogenic miRNA highly expressed in B-cell malignancies, particularly in the non–germinal center B-cell or activated B-cell subtype of diffuse large B-cell lymphoma (ABC-DLBCL), where it is considered a potential diagnostic and prognostic biomarker. Thus, miR-155 inhibition represents an important therapeutic strategy for B-cell lymphomas. In this study, we tested the efficacy and pharmacodynamic activity of an oligonucleotide inhibitor of miR-155, cobomarsen, in ABC-DLBCL cell lines and in corresponding xenograft mouse models. In addition, we assessed the therapeutic efficacy and safety of cobomarsen in a patient diagnosed with aggressive ABC-DLBCL.

Corresponding Author: Frank J. Slack, BIDMC, 330 Brookline Avenue, Boston, MA 02215. Phone: 617-735-2601; Fax: 617-735-2646; fslack@bidmc.harvard.edu.

Authors' Contributions

E. Anastasiadou: Conceptualization, data curation, software, formal analysis, supervision, validation, investigation, visualization, methodology, writing-original draft, writing-review and editing. **A.G. Seto:** Conceptualization, resources, data curation, software, formal analysis, supervision, validation, investigation, visualization, methodology, writing-review and editing. **X. Beatty:** Data curation, software, validation, investigation. **M. Hermreck:** Formal analysis, validation, writing-review and editing. **M.-E.Gilles:** Data curation, software, formal analysis. **D. Stroopinsky:** Data curation, investigation. **L.C. Pinter-Brown:** Data curation, formal analysis, investigation, visualization, writing-review and editing. **L. Pestano:** Data curation, investigation, writing-review and editing. **C. Marchese:** Writing-review and editing. **D. Avigan:** Investigation, writing-review and editing. **P. Trivedi:** Investigation, writing-review and editing. **D. M. Escolar:** Resources, data curation, supervision, writing-review and editing. **A.L. Jackson:** Resources, data curation, investigation, writing-review and editing. **F.J. Slack:** Conceptualization, resources, data curation, supervision, funding acquisition, investigation, methodology, project administration, writing-review and editing.

The costs of publication of this article were defrayed in part by the payment of page charges. This article must therefore be hereby marked *advertisement* in accordance with 18 U.S.C. Section 1734 solely to indicate this fact.

Note: Supplementary data for this article are available at Clinical Cancer Research Online (http://clincancerres.aacrjournals.org/).

Experimental Design: Preclinical studies included the delivery of cobomarsen to highly miR-155–expressing ABC-DLBCL cell lines to assess any phenotypic changes, as well as intravenous injections of cobomarsen in NSG mice carrying ABC-DLBCL xenografts, to study tumor growth and pharmacodynamics of the compound over time. To begin to test its safety and therapeutic efficacy, a patient was recruited who underwent five cycles of cobomarsen treatment.

Results: Cobomarsen decreased cell proliferation and induced apoptosis in ABC-DLBCL cell lines. Intravenous administration of cobomarsen in a xenograft NSG mouse model of ABC-DLBCL reduced tumor volume, triggered apoptosis, and derepressed direct miR-155 target genes. Finally, the compound reduced and stabilized tumor growth without any toxic effects for the patient.

Conclusions: Our findings support the potential therapeutic application of cobomarsen in ABC-DLBCL and other types of lymphoma with elevated miR-155 expression.

Introduction

Diffuse large B-cell lymphoma (DLBCL) accounts for approximately 30%–58% of all non-Hodgkin lymphomas (NHL). On the basis of gene expression and IHC profiling within the B-cell lineage, there are two main molecular subtypes, namely, the germinal center B-cell (GCB)-derived DLBCL and the non-GCB or activated B-cell (ABC) type (1, 2). The incidence of the latter type is approximately 40% of all DLBCL cases with higher incidence in the elderly (3, 4). More recent studies have explored the genomic landscape of DLBCL by whole-exome, targeted amplicons, and transcriptomic sequencing to specifically identify combinations of genetic changes (5, 6). Through an improved distinction of different genomic subgroups of DLBCLs, these two groundbreaking studies have enabled improved risk stratification before the patients receive the standard chemotherapy or immunotherapy. Generally, patients with ABC-DLBCL have a worse prognosis, usually owing to higher expression of *BCL2, BCL6*, and *MYC* oncogenes (7–9). The standard treatment is a cocktail of the chemotherapeutic drugs cyclophosphamide, doxorubicin, vincristine, and prednisone combined with rituximab mAbs (R-CHOP), followed by radiotherapy or surgery. A selective efficacy of R-CHOP in combination with ibrutinib or lenalidomide has also been reported previously (10, 11). Although chemotherapy prolongs the survival of patients with DLBCL, relapse and drug resistance are not uncommon and may occur in as many as 40% of patients (12). Particularly, the complete response (CR) rate in patients with ABC-type DLBCL to R-CHOP chemotherapy is only 30% while a higher CR rate of 70% is observed in patients with GC-type DLBCL (3, 13).

miRNAs are 20–22 nucleotide long noncoding RNAs, which inhibit the translation of genes that participate in a variety of biological processes including differentiation, inflammation, immunity, and tumorigenesis (14). Among known miRNAs involved in cancer, increased miR-155 expression is crucial for B-cell lymphoma initiation and progression (15–17). Thus, miR-155 has emerged as a diagnostic and prognostic marker as well as a therapeutic target in B-cell malignancies including DLBCL (18, 19). The primary transcript from which the mature miR-155 is processed, the B-cell integration cluster (BIC), is also highly expressed in Hodgkin and NHL (20). In particular, the NFκB binds to the BIC promoter, and might induce miR-155 expression. Because NFκB is constitutively activated in ABC-

DLBCL rather than in the GC subtype, this might explain higher miR-155 expression in ABC-DLBCL (21, 22). Furthermore, high expression of miR-155 in E(mu)-mmu-miR155 transgenic mice was sufficient to develop a lymphoproliferative disease that resembles human acute lymphoblastic leukemia or high-grade lymphomas (23). MiR-155-expressing lymphomas display features of oncogene addiction, epitomized in the doxycycline Tet-Off-based mouse model miR-155^{LSLtTA} (24, 25).

Several other *in vitro* and *in vivo* studies point to miR-155 as a *bona fide* pharmacologic target of miRNA-based therapy in lymphoma (18). In a recent study, inhibition of miR-155 using cobomarsen in cutaneous T-cell lymphoma (CTCL) cell lines derepressed miR-155 target genes, decreased proliferation and induced apoptosis (26). Based in part on these results, cobomarsen is being assessed in a phase II clinical trial for the treatment of CTCL, mycosis fungoides subtype (MF-CTCL), (https://clinicaltrials.gov/ct2/show/study/NCT03713320).

Over the years, it has become apparent that miR-155 may represent a therapeutic target especially in the ABC-type DLBCL, where the estimated CR rate to conventional therapeutic management is still very low, underlining the importance of developing novel therapeutic strategies (12). Given the role of miRNA deregulation in cancer and particularly of miR-155 in DLBCLs, in this study, we investigated the effect of cobomarsen in ABC-DLBCL cell lines with high miR-155 expression (27). In addition, *in vivo* efficacy of cobomarsen was tested in xenografts and in a patient with aggressive DLBCL.

Materials and Methods

Cells

ABC-type DLBCL cell lines, U2932, OCI-LY3, and RCK8 were purchased from DSMZ and were grown in a RPMI1640 medium supplemented with 10% FBS without antibiotics and kept in a 37°C, 5% CO_2 incubator. All cell lines were *Mycoplasma* free tested with MycoAlert mycoplasma detection kit (LONZA). ABC-type DLBCL cell lines were chosen because of their high miR-155 expression, compared with normal CD19$^+$ B cells.

Oligonucleotide

Cobomarsen is a single-stranded, chemically modified miR-155–targeting oligonucleotide. Cobomarsen and its corresponding FITC-conjugated variant were synthesized and purified by miRagen Therapeutics. A *Caenorhabditis elegans* anti-miRNA that does not target any mammalian miRNA is used throughout as control oligonucleotide (26).

qRT-PCR

Total RNA was isolated from 3×10^6 cells from each cell line using Direct-zol RNA MiniPrep Plus Kit (Zymo Research) according to manufacturer's instructions. We used commercially available Human B Cell (CD19$^+$) total RNA isolated from highly purified human CD19$^+$ B lymphocytes, derived from multiple healthy donors (Miltenyi biotec Inc., catalog no. 130–093-169). The integrity of RNA was routinely checked using 1% agarose gel and RNA quantification was estimated with a DS-11 spectrophotometer (DeNovix).

Synthesis of cDNA was performed by retro-transcribing 1 μg RNA with Super-Script IV First-Strand Synthesis System (Invitrogen) according the manufacturer's instructions. For miR-155 detection, 1 μg RNA was retro-transcribed with miScriptII RT Kit (QIAGEN).

RNA extraction from mice xenografts was performed using the RNeasy Plus 96 Kit, (Qiagen, catalog no. 74192) according to the manufacturer's instructions. Nine μL of the isolated RNA were subjected to reverse transcription using the High Capacity cDNA Reverse Transcription Kit (Applied Biosystems, catalog no. 4368813). Additional details of qRT-PCR conditions can be found in Supplementary Materials and Methods.

Cobomarsen delivery verification

Two different concentrations, 2.5 and 10 μmol/L of FITC-conjugated cobomarsen were delivered without any transfection reagent into 5×10^4 U2932 cells in a 12-well plate for 6 hours. Cobomarsen positive cells were detected by flow cytometry using a Gallios flow analyzer (Beckman Coulter).

Visualization of the compound (2.5 μmol/L) in U2932 cells 48 hours postdelivery was performed with Zeiss LSM 880 Confocal Microscope. Further details can be found in the Supplementary Materials and Methods.

miR-155 luciferase reporter

To verify whether cobomarsen can suppress endogenous miR-155 activity, U2932, OCI-LY3, and RCK8 cells were seeded one day before transfection with psiCHECK-2 miR-155 biosensor at a concentration of 2×10^5 cells per well in triplicates in a 24-well plate. A total of 20 ng psiCHECK-2 miR-155 biosensor was transfected with DharmaFECT Duo Transfection Reagent (Dharmacon), as described previously (25). Twenty-four hours posttransfection, culture medium was carefully removed from each well and replenished with 1.5 mL/well of fresh medium containing 10 μmol/L cobomarsen or 10 μmol/L control oligonucleotide and in the absence of any transfection reagent. Twenty-four hours later, the relative luminescence units (RLU) of miR-155 luciferase activity was detected with Dual luciferase reporter assay (Promega) and recorded with GloMax explorer instrument (Promega), according to the manufacturer's instructions. The experiment was repeated at least three times. Further details are in Supplementary Materials and Methods.

Cell proliferation assay

Cobomarsen or oligonucleotide control transfected cells (2×10^4 per well) were placed in triplicate, in a 96 opaque-walled flat well plates for cell culture to estimate cell proliferation over time. At 48, 72, and 96 hours postdelivery of the compounds, 100 μL of CellTiter-Glo Reagent (Promega) was added in each well, according to the manufacturer's instructions. The experiment was repeated at least three times. Further details are described in the Supplementary Materials and Methods.

Apoptosis assay by Annexin V/propidium iodide

To study whether cobomarsen has any effect on apoptosis in DLBCL cell lines with high levels of miR-155, 10 μmol/L control oligonucleotide or cobomarsen was added directly to 2

mL of cell culture medium containing 5×10^5 U2932, OCI-LY3, and RCK8 cells in a 6-well plate. The cell culture medium was replenished with fresh medium containing the corresponding oligonucleotide at 48 hours to sustain viability. After 96 hours, one million cells from each cell line were harvested, washed in PBS, and stained for apoptosis according to APC Annexin V Apoptosis Detection with PI Kit instructions (Bio-Legend). Detection of the percentage of early apoptotic (only Annexin V positive), late apoptotic [both Annexin V/propidium iodide (PI) positive], and necrotic cells (only PI) was performed using a Gallios flow analyzer (Beckman Coulter). Data were analyzed with Kaluza for Gallios Software (28). The experiment was repeated three times for each cell line.

DLBCL xenografts in mice

Five-to-six weeks old female NSG (*NOD*.Cg-Prkdc^{scid} Il2rg^{tm1Wjl}/SzJ, strain no. 005557) mice were purchased from The Jackson laboratory and were maintained at the BIDMC mouse facility in accordance with the Institutional Animal Care and Use Committee (IACUC) guidelines. Ten million U2932 cells were injected subcutaneously on the left flank of 54 mice included in the tumor growth and pharmacodynamic studies. After 9–12 days, when the tumor volume reached a range of 100–200 mm^3, the mice were randomized into groups based on the mean of their tumor volumes and the SD between the groups. This was done to ensure an even distribution of tumor volumes on the first day of treatment. Treatments were performed through intravenous injections in the tail vein, using a 27-gauge syringe. For the tumor growth study, a total of 24 mice were divided into four treatment groups (Table 1).

Group A contained 12 mice treated with 100 μL of PBS. Group B contained 12 mice treated with 100 μL PBS containing 1 mg/mL cobomarsen. To ensure that the control oligo did not have any impact on the tumor growth, group C and D contained 3 mice each treated respectively with 100 μL PBS and 100 μL PBS contained 1 mg/mL cobomarsen. For the pharmacodynamic study, 24 mice were divided into four groups, 8 mice each treated with 100 μL PBS (group 1), 1mg/kg control oligo (group 2) and 1 mg/kg cobomarsen (group 3; Table 2). Tumor volume was measured with an electronic caliper at baseline and prior to each intravenous injection. According to the IACUC guidelines, once the tumor volume in the control groups, (PBS or control oligo groups) has reached 2,000 mm^3, all mice were euthanized. The number of animals treated with cobomarsen, control oligonucleotide, or vehicle/PBS in studies assessing tumor growth and pharmacodynamic effects can be found in Tables 1 and 2, respectively. Tumor volumes were calculated from digital caliper raw data by using the formula: Volume (mm^3) = (tumor length × tumor width^2)/2 every 2 days. During the study, no animal distress or weight lost was observed.

Detection of cobomarsen by S1 nuclease protection assay in the xenografts

Tumor tissue samples were prepared at 100 mg/mL in 3 mol/L GITC buffer (3 mol/L guanidine-isothiocyanate, 0.5 mol/L NaCl, 0.1 mol/L Tris, pH 7.5, and 10 mmol/L EDTA) by homogenizing with an MP FastPrep-24 tissue homogenizer at a speed setting of 6.0, using two 30-second runs. Tissue homogenates and plasma were diluted in 1 mol/L GITC Buffer for testing. Fully complementary 5′ biotinylated probes with 3′ FITC residues were

synthesized and used to capture cobomarsen analyte using 96-well streptavidin coated plates (Roche). Further details are described in the Supplementary Materials and Methods.

TUNEL assay

From the study assessing pharmacodynamic effects (Table 2), tumors were obtained from 3 mice per group, at 96 hours posttreatment with either PBS alone, 1 mg/kg control oligonucleotide or 1 mg/kg cobomarsen. Tumor (tissue) slices were embedded in optimal cutting temperature compound in cryomolds. Cryosections and TUNEL Chromogenic Apoptosis Detection, kit purchased from Genecopoeia, were performed by the Histology Core of Beth Israel Deaconess Medical Center (Boston, MA). The TUNEL-positive area was quantified with ImageJ software. Phase-contrast images were acquired with OLYMPUS BX51 microscope (software DP2-BSW) with 4× and 20× objective. Supplementary Information contains further details of the method.

Patient selection criteria

A patient was recruited as part of the clinical trial of safety, tolerability, and pharmacokinetics of cobomarsen in patients with MF-CTCL, DLBCL, or adult T-cell leukemia/lymphoma (ATLL; number NCT02580552), based on the following inclusion criteria: for patients with biopsy-proven DLBCL who are intolerant to, or have disease that is relapsed/refractory after at least two prior therapies, including any anti-CD20 mAband chemotherapy with curative intent. The patient is a 61-year-old female with diabetes, low B12, and peripheral neuropathy who was diagnosed when she presented with left tonsillar enlargement and the biopsy of her tonsillar mass showed DLBCL. The cell of origin of the DLBCL was non-GCB/ABC subtype.

The investigators obtained written consent from the patient and the study was performed after approval by institutional review boards of University of California, Irvine, CA. This study was conducted in compliance with the International Conference on Harmonization (ICH) Good Clinical Practice Guidelines; U.S. Code of Federal Regulations (CFR), clinical studies (21 CFR § 50, 56, 312); the Declaration of Helsinki, and with ICH guidelines regarding scientific integrity (E4, E8, E9, and E10).

Therapeutic regimens used for the patient

Prior to cobomarsen clinical trial enrollment, the patient was treated with five regimens, as detailed in Supplementary Table S1.

After the fifth line of treatment, the patient was enrolled in the cobomarsen study, according to the inclusion and exclusion criteria for the clinical trial. The patient was administered 600 mg i.v. infusion of cobomarsen for five cycles, each cycle covered 28 days. Physical exams and injections were performed in the same day, as follows: first cycle, six injections at days 1, 3, 5, 12, 19, 26; second, third, and fourth cycle, four injections/cycle scheduled at days 1, 8, 15, 22; fifth cycle, three injections at days 1, 8, 15. The nodal tumor mass' longest axis (in cm) measurements were performed at the same indicated days with rulers, because repeated scans of the patient over time were not possible.

Statistical analysis

For the in *vivo* experiments, we performed a power analysis to estimate the group size of NSG mice to obtain statistically significant differences between the cobomarsen treated and control groups. All statistical analyses were performed with PRISM7. The statistical significance of the mean value of the tumor volumes in different time points between the groups of mice was performed using two-way Anova with Sidak multiple comparisons test.

Unpaired, two-tailed *t* test analysis was performed for gene expression studies *in vitro*, and for the TUNEL assay.

Results

Expression of miR-155 in ABC-DLBCL cell lines

Several studies have shown that miR-155 is generally highly expressed in patients with ABC-DLBCL in comparison with healthy controls (29–31). Therefore, we first assessed miR-155 expression in three human ABC-DLBCL cell lines, U2932, OCI-LY3, and RCK8, by qRT-PCR. As expected, all three cell lines expressed high levels of miR-155 (Fig. 1A), while the expression of three experimentally validated miR-155 target genes, *HIVEP2, TP53INP1*, and *MAFB* (25), was significantly reduced (Fig. 1B) compared with $CD19^+$ B cells. Furthermore, we showed that miR-155 expression was higher in the ABC-DLBCL compared with three GC-DLBCL cell lines (Supplementary Fig. S1).

Cobomarsen delivery in DLBCL cell lines

To verify functional uptake of the compound, we first transfected cells with a miR-155 biosensor, a plasmid which contains a complementary sequence to the mature miR-155 inserted downstream of the *luc* gene. This reporter results in suppression of luciferase expression when the target sequence is bound by endogenous miR-155. Twenty-four hours following transfection of cells with the miR-155 biosensor and after a careful removal of the supernatant, we treated the cell cultures with 10 μmol/L of cobomarsen or a control oligonucleotide by adding the compounds directly to the culture medium. Luciferase activity was measured 24 hours later. Inhibition of endogenous miR-155 by cobomarsen will prevent the binding of miR-155 to the seed region within the biosensor, which will result in derepression (increased expression) of the luciferase reporter. As shown in Fig. 2A, luciferase activity was significantly derepressed by cobomarsen in all cell lines compared with the control oligo treatment. These data demonstrate that functional uptake and target engagement by passive delivery of cobomarsen in DLBCL cell lines is efficient even in the presence of higher amounts of miR-155 in the OCI-LY3 and RCK8 cell lines.

Furthermore, to assess the dose dependence and sequence specificity on miR-155 activity, we treated all three cell lines with three different concentrations of cobomarsen: 2.5, 5, and 10 μmol/L and subsequently we examined the expression of four previously experimentally validated miR-155 target genes, *BACH1, INPP5D, TP53INP1*, and *HIVEP2* (25, 32) (Supplementary Fig. S2). Our results showed that 10 μmol/L cobomarsen treatment of U2932 cell line provided a higher fold change of derepression of these miR-155 target genes, thus we continued our experiments in U2932 cell line (Supplementary Fig. S2A). To

estimate the cobomarsen uptake, U2932 cells were treated with 2.5 and 10 μmol/L FITC-conjugated compound and analyzed by flow cytometry. As shown in Fig. 2B, at 2.5 and 10 μmol/L, the FITC mean fluorescence intensity (MFI) was higher compared with the untreated cells, within 6 hours, which is indicative that cells have started to take up the compound. Furthermore, internalization of FITC conjugated compound could be obtained even at the lowest concentration, (2.5 μmol/L) as seen at 48 hours postdelivery (Fig. 2C). A higher magnification of cobomarsen FITC-positive cells clearly enabled us to visualize the compound in the cytoplasm and excluded from the nucleus (Fig. 2D). These results show that the compound can be delivered and that it is active inside the cells because it can bind to its target and inhibit it from acting on the complementary sequence of the miR-155 biosensor.

Phenotypic impact of cobomarsen on proliferation and apoptosis in DLBCL cell lines

Several studies have shown that inhibition of miR-155 in lymphoma/leukemia and DLBCL reduces cell proliferation and induces apoptosis (24, 33). Therefore, we assessed cell proliferation over time in cobomarsen-treated ABC-DLBCL cell lines, in comparison with the control oligonucleotide-treated cells. Cells were treated with 10 μmol/L cobomarsen for 96 hours and the luminescence values of metabolically viable cells were estimated at 48, 72, and 96 hours (Fig. 3A). There was a reduction of the luminescence signal, normalized to the control oligonucleotide-treated cells, which is directly proportional to the reduction of cellular ATP levels, indicating a decrease in cell proliferation. To examine whether the decrease in proliferation was due to increased apoptosis, all three cell lines were treated with the same amount (10 μmol/L) of cobomarsen. Indeed, cobomarsen triggered a significant induction of late apoptosis in all cell lines at 96 hours posttreatment (Fig. 3B). In U2932 and OCI-LY3 cells, treatment with the control oligonucleotide also induced a marginal increase of late apoptotic cells, compared with the untreated cell line. However, the magnitude of effect and the significance of the increased apoptosis were greater with cobomarsen treatment in all cell lines. Collectively, these data demonstrate that inhibition of miR-155 with cobomarsen results in decreased proliferation and increased apoptosis of DLBCL cells.

Cobomarsen inhibits tumor growth *in vivo*

To determine whether cobomarsen can impact tumor growth *in vivo*, we established xenografts of DLBCL cells expressing high levels of miR-155. While miR-155 expression was elevated in three DLBCL cell lines (Fig. 1A), higher expression was observed in OCI-LY3 and RCK8 cells. We selected U2932 for xenograft experiments because RCK8 cells did not engraft in mice and OCI-LY3 cells grew too quickly to assess the effect of miR-155 inhibition on tumor growth. Most importantly, we observed that miR-155 target gene derepression was more pronounced in U2932 cell line treated with cobomarsen, compared with the other two cell lines (Supplementary Figs. S2 and S3). Twelve mice each in group A and B, as well as three mice each in group C and D, were intravenously inoculated according to the details described in Table 1 and on days 0, 2, 4, and 7 following enrollment into the study, as shown in the experimental timeline (Fig. 4A). Tumor volume was measured 3 days after the last dose or until the tumor volume reached 2,000 mm^3, until mice were euthanized. Intravenous administration of 1 mg/kg cobomarsen reduced tumor growth in group B compared with group A control mice treated with PBS, most significantly at day 7 (**, $P =$

0.0019) and day 10 (****, $P < 0.0001$; Fig. 4B). In contrast, there was no impact of the control oligo on tumor volume (group D) in comparison with PBS only treated group C mice (Fig. 4C). Both cobomarsen and the control oligonucleotide were well tolerated and no adverse events were observed.

Cobomarsen derepresses miR-155 target gene expression *in vivo* and *in vitro*

To understand the molecular mechanisms that underlie the reduction of tumor growth by cobomarsen, we assessed whether miR-155 target genes were derepressed after cobomarsen treatment. The experimental timeline of cobomarsen-treated xenografts used to assess pharmacodynamic effects of cobomarsen is shown in Fig. 5A. Mice were inoculated with 10 million U2932 cells in the right flank. Mice received two intravenous injections of either PBS alone (vehicle), 1 mg/kg cobomarsen or 1 mg/kg control oligonucleotide on days 0 and 2 following enrollment into the study. Before commencement of the treatment, we ensured that the tumor volume average and SD were similar among the three groups. Tumor tissue was harvested 24 hours after the last dose and either processed to evaluate miR-155 target gene expression or embedded for cryosections to perform the TUNEL assay. The TUNEL assay showed that there are more apoptotic cells (dark brown staining) in the tumor tissues of cobomarsen-treated mice, compared with the PBS and control oligonucleotide groups (Fig. 5B). Furthermore, the distribution of cobomarsen to all eight xenografts was successfully detected using a hybridization assay (Fig. 5C).

A panel of 12 experimentally validated miR-155 target genes, was investigated by qPCR (Fig. 5D): *MAFB, SH3PXD2A, SOCS1* (34), *CUX1, WEE1, BACH1, INPP5D, HIVEP2, TP53INP1* (25, 35), *JARID, PICALM* (26), *CSFR1* (36). Upon cobomarsen treatment, there was a significant derepression of miR-155 target genes, such as *Cut Like Homeobox 1 (CUX1;* number 3), *(SH3 And PX Domains 2A*) *SH3PXD2A, (number 7) Suppressor Of Cytokine Signaling 1 (SOCS1;* number 8) and *WEE1 G2 Checkpoint Kinase (WEE1;* number 10), between the PBS-treated mice comparing with the control oligonucleotide and to the cobomarsen-treated group of mice (Fig. 5D).

Next, we investigated whether the derepression of miR-155 targets observed in cobomarsen-treated mice can be recapitulated in three DLBCL cell lines. Two target genes, namely, *WEE1* and *CUX1*, were consistently derepressed in both mice and in cell lines (Fig. 5D and E). The rest of the genes were variably derepressed in the two systems (Fig. 5D; Supplementary Fig. S3). For instance, while *SOCS1* and *SH3PXD2A* were significantly derepressed in cobomarsen-treated mice, their expression did not change in the three DLBCL cell lines. The expression of *CUX1* was significantly altered in U2932 and OCI-LY3 but not in RCK8 (Fig. 5E).

Cobomarsen as monotherapy

The patient was enrolled immediately [as she had progressive disease (PD)] in the clinical trial of cobomarsen (https://clinicaltrials.gov/ct2/show/NCT02580552). The details of patient's prior treatment history and outcome is shown in the Supplementary Material and Methods section. At this time, a radiographic evaluation showed that the patient had developed adenopathy in the right cervical, right parotid, right external iliac, and right

inguinal areas. On day 3 of the trial, the patient noted that immediately after the first intravenous injection (600 mg), her right neck mass rapidly increased then decreased in size on the same day. At cycle 1, day 3, physical examination of her right neck node measured 3.5 cm and her right inguinal node measured 3.0cm (Fig. 6). By cycle 2, day 1, the right neck node was no longer palpable; however, the right inguinal area was noted to be swollen to 6.0 cm without a definite palpable mass. Two weeks later, on cycle 2, day 15, the right neck remained not palpable and the right inguinal mass had decreased to 2.0 cm. The right inguinal mass continued to decrease until cycle 2, day 27, when there were no palpable nodes found during the physical exam. By cycle 3, day 14, a right supraclavicular node was palpable and measured 1.5 cm. On protocol-mandated CT scanning, the patient had PD because of a new right paratracheal node of 1.4 cm, but all other nodes were stable. A right neck fine needle aspiration documented the presence of DLBCL, and at the end of treatment, the patient developed her first elevated lactate dehydrogenase and increasing lymphadenopathy in the left inguinal and left supraclavicular nodes. The patient was discontinued from the cobomarsen clinical trial after 21 total doses of cobomarsen through five cycles, as noted in the clinical database (miRagen trial number: MRG106–11-101 and NCT02580552). The reason for discontinuation was documented as early termination due to disease progression, according to the clinical trial criteria.

Subsequent to trial participation, the patient had rapidly PD and received one dose of bendamustine in combination with rituximab. The patient then received chimeric antigen receptor T-cell (CAR-T) therapy with an initial radiographic complete response but PD 3 months after CAR-T infusion. The patient received ibrutinib in combination with rituximab for 3 months with PD and is currently experiencing a partial response after four doses of polatuzumab in combination with rituximab. She was then treated with polatuzumab achieving a partial response after cycle 4 but PD after cycle 6. The patient has been offered hospice services. As seen by the patient’s rapid course after discontinuation of cobomarsen, cobomarsen appeared to reduce the size of sometimes bulky adenopathy demonstrably on physical examination, and stabilize the disease.

Discussion

OncomiR-155 expression is highly induced in B-cell lymphoproliferative disorders and in DLBCL, especially in the ABC subtype and it is considered a biomarker for these malignancies (30, 32, 37). Nevertheless, miRNA-based therapies for cancer treatment are challenging, due to their unfavorable physicochemical properties that may prevent their cellular uptake and distribution in various tissues. Furthermore, miRNA-based therapies may be unstable in plasma and tissues due to the presence of nucleases and endosomal sequestration (18, 38, 39). To overcome these issues, chemical modifications of RNAs have been incorporated into anti-miRNAs that target oncogenic miRNAs or miRNA mimics that represent tumor-suppressive miRNAs to enhance delivery and distribution in the tumor tissue (24, 40, 41). Because of the improvements in delivery approaches and stability of miRNA compounds, clinical trials with such compounds to treat cancer could certainly pave the way for better therapeutic options (42).

One of the first promising anti-miR-155 oligonucleotides for therapeutic purpose was an 8-mer locked nucleic acid (LNA) anti-miR-155, delivered systemically in a xenograft mouse model of Waldenstrom macroglobulinemia that decreased tumor growth (34). However, this oligonucleotide has not yet entered into clinical trials. In our study, we assessed cobomarsen, an LNA-based anti-miR-155 compound, in DLBCL, which is now being assessed in a phase II clinical trial for the treatment of CTCL (https://clinicaltrials.gov/ct2/show/study/NCT03713320). We introduced cobomarsen into human ABC-DLBCL cell lines (with high miR-155 expression), without the assistance of any delivery agent. The anti-miR-155 compound reduced proliferation and induced apoptosis *in vitro*. In addition, the compound reduced tumor growth of U2932 cell line engraftments in NSG mice. These phenotypic effects were associated with derepression of miR-155 target genes, both *in vitro* and *in vivo*.

Very little is known about how miR-155 influences WEE1 and CUX1 in human DLBCL cell lines (34, 43). Interestingly, a previous study from our group by Cheng and colleagues, showed thatCUX1and WEE1 mRNAs were among miR-155–predicted targets (25). In the same study, it was shown that CUX1 expression is derepressed after withdrawal of miR-155 in mir-155^{LSLtTA} mice when treated with doxycycline. Our results are consistent with the observations by Cheng and colleagues CUX1 is an evolutionarily conserved transcription factor with two isoforms with diverse functions. Indeed, it acts as a tumor suppressor gene in myeloid neoplasms by regulating cell-cycle genes, but its altered expression may also lead to tumor progression (44). Our study demonstrates that there is an induction of cell death upon delivery of cobomarsen *in vitro* and *in vivo*. Further investigation is needed to specifically implicate CUX1 in the reduction of tumor growth.

WEE1, a G_2–M checkpoint tyrosine kinase, catalyzes the inhibitory tyrosine phosphorylation of CDC2/cyclin B kinase. This in turn inhibits mitosis in cells that have damaged genomes and may induce DNA repair or result in cell death (45). Tili and colleagues have shown that increased expression of miR-155 in breast cancer cell lines induced the proliferation rate by targeting WEE1 transcripts (35). Inhibition of miR-155 with an antisense oligonucleotide in primary B cells of Eμ-miR-155 transgenic mice and in breast cancer cell lines released WEE1 expression and caused a block in G_2–M transition. In DLBCLs, we find a significant derepression of WEE1 upon cobomarsen delivery. This is consistent with a tumor-suppressive role of the WEE1 gene and confirms the oncogenic nature of miR-155. However, further experiments are needed to conclusively demonstrate the direct tumor suppressive role of WEE1 in DLBCL.

As mentioned previously, cobomarsen is currently being tested in a first-in-human phase II clinical trial in patients with MF-CTCL, https://clinicaltrials.gov/ct2/show/study/NCT03713320. In addition, a study showed that cobomarsen had antiproliferative, proapoptotic effects in MF and human lymphotropic virus type 1 (HTLV-1+) CTCL cell lines *in vitro* (26). Another phase I clinical trial (https://clinicaltrials.gov/ct2/show/NCT02580552) is currently evaluating cobomarsen-treated patients with ATLL, CLL. We have begun to assess the safety and therapeutic utility of cobomarsen, particularly for a relapsing case of ABC-DLBCL. A patient affected by ABC-DLBCL previously treated with chemotherapeutic regimens but relapsing, was enrolled for cobomarsen treatment. In contrast with other therapeutic strategies, cobomarsen treatment resulted in a significant

decrease of tumor nodes with apparently no side effects. To our knowledge, this is the first miRNA-based therapy that had beneficial outcome for the patient with no toxicity. This level of disease stabilization with minimal toxicity is uncommon for an investigational agent in the face of a very aggressive B-cell lymphoma. Clearly, these findings need to be confirmed in more patients in the future clinical trial to better evaluate pharmacodynamics and safety of cobomarsen therapy against hard-to treat lymphomas.

Several reports suggest that miR-155 is deregulated in virus-infected lymphomas like Burkitt lymphoma. It is known that Epstein–Barr virus alters cellular miRNA expression in B lymphomas (46–51). Other viruses like HHV-8 and Marek disease virus have a viral miRNA homolog of miR-155 with identical seed sequence (52). This suggests that deregulation of either cellular miR-155 or its viral miRNA orthologues is important for virus-associated lymphomas (53). Our study could extend the therapeutic potential of cobomarsen for such lymphomas as well.

In conclusion, more effective therapies are urgently needed to cure refractory or relapsed DLBCL. Our preclinical studies support the use of cobomarsen for the treatment of patients with DLBCL with high miR-155, for the therapeutic management of patients with DLBCL. The results observed here, in 1 patient only, might provide impetus for the continuation and extension of cobomarsen-based therapy not only for ABC-DLBCLs but other lymphomas with high miR-155 expression.

Supplementary Material

Refer to Web version on PubMed Central for supplementary material.

Acknowledgments

This study was supported by a sponsored research agreement from miRagen Therapeutics to F.J. Slack. The authors also acknowledge the support of the Ludwig Institute at Harvard and the NCI Outstanding Investigator Award (R35CA232105) to F.J. Slack, and the V Foundation Award to F.J. Slack and D. Avigan.

Authors' Disclosures

A.G. Seto reports a patent for US 9,771,585 issued. L.C. Pinter-Brown reports personal fees from Miragen during the conduct of the study and personal fees from Miragen outside the submitted work. L. Pestano reports other from miRagen Therapeutics during the conduct of the study and other from miRagen Therapeutics outside the submitted work. D. Avigan reports grants from V foundation during the conduct of the study, as well as personal fees from Takeda, BMS, Karyopharm, Chugai, Kite, Legend, Parexel, and Janssen; grants and personal fees from Celgene; and grants from Pnarmacyclics outside the submitted work. D.M. Escolar reports other from miRagen Therapeutics during the conduct of the study and other from miRagen Therapeutics outside the submitted work. A.L. Jackson reports a patent for miR-155 inhibitors in CTCL issued; and A.L. Jackson was an employee and stockholder in Miragen Therapeutics at the time the work was performed. F.J. Slack reports grants and nonfinancial support from miRagen Rx during the conduct of the study. No disclosures were disclosed by the other authors.

References

1. Alizadeh AA, Eisen MB, Davis RE, Ma C, Lossos IS, Rosenwald A, et al. Distinct types of diffuse large B-cell lymphoma identified by gene expression profiling. Nature 2000;403:503–11. [PubMed: 10676951]
2. Li S, Young KH, Medeiros LJ. Diffuse large B-cell lymphoma. Pathology 2018;50: 74–87. [PubMed: 29167021]

3. Sehn LH, Berry B, Chhanabhai M, Fitzgerald C, Gill K, Hoskins P, et al. The revised International Prognostic Index (R-IPI) is a better predictor of outcome than the standard IPI for patients with diffuse large B-cell lymphoma treated with R-CHOP. Blood 2007;109:1857–61. [PubMed: 17105812]
4. Nowakowski GS, Czuczman MS. ABC, GCB, and double-hit diffuse large B-cell lymphoma: does subtype make a difference in therapy selection? Am Soc Clin Oncol Educ Book 2015:e449–57. [PubMed: 25993209]
5. Chapuy B, Stewart C, Dunford AJ, Kim J, Kamburov A, Redd RA, et al. Molecular subtypes of diffuse large B cell lymphoma are associated with distinct pathogenic mechanisms and outcomes. Nat Med 2018;24:679–90. [PubMed: 29713087]
6. Schmitz R, Wright GW, Huang DW, Johnson CA, Phelan JD, Wang JQ, et al. Genetics and pathogenesis of diffuse large B-cell lymphoma. N Engl J Med 2018; 378:1396–407. [PubMed: 29641966]
7. Horn H, Ziepert M, Becher C, Barth TF, Bernd HW, Feller AC, et al. MYC status in concert with BCL2 and BCL6 expression predicts outcome in diffuse large B-cell lymphoma. Blood 2013;121:2253–63. [PubMed: 23335369]
8. Visco C, Tzankov A, Xu-Monette ZY, Miranda RN, Tai YC, Li Y, et al. Patients with diffuse large B-cell lymphoma of germinal center origin with BCL2 translocations have poor outcome, irrespective of MYC status: a report from an International DLBCL rituximab-CHOP Consortium Program Study. Haematologica 2013;98:255–63. [PubMed: 22929980]
9. Tilly H, Gomes da Silva M, Vitolo U, Jack A, Meignan M, Lopez-Guillermo A, et al. Diffuse large B-cell lymphoma (DLBCL): ESMO Clinical Practice Guidelines for diagnosis, treatment and follow-up. Ann Oncol 2015;26:v116–25. [PubMed: 26314773]
10. Younes A, Thieblemont C, Morschhauser F, Flinn I, Friedberg JW, Amorim S, et al. Combination of ibrutinib with rituximab, cyclophosphamide, doxorubicin, vincristine, and prednisone (R-CHOP) for treatment-naive patients with CD20-positive B-cell non-Hodgkin lymphoma: a non-randomised, phase 1b study. Lancet Oncol 2014;15:1019–26. [PubMed: 25042202]
11. Nowakowski GS, LaPlant B, Macon WR, Reeder CB, Foran JM, Nelson GD, et al. Lenalidomide combined with R-CHOP overcomes negative prognostic impact of non-germinal center B-cell phenotype in newly diagnosed diffuse large B-Cell lymphoma: a phase II study. J Clin Oncol 2015;33:251–7. [PubMed: 25135992]
12. Vaidya R, Witzig TE. Prognostic factors for diffuse large B-cell lymphoma in the R(X)CHOP era. Ann Oncol 2014;25:2124–33. [PubMed: 24625454]
13. Coiffier B, Sarkozy C. Diffuse large B-cell lymphoma: R-CHOP failure-what to do? Hematology Am Soc Hematol Educ Program 2016;2016:366–78. [PubMed: 27913503]
14. Anastasiadou E, Jacob LS, Slack FJ. Non-coding RNA networks in cancer. Nat Rev Cancer 2018;18:5–18. [PubMed: 29170536]
15. Higgs G, Slack F. The multiple roles of microRNA-155 in oncogenesis. J Clin Bioinforma 2013;3:17. [PubMed: 24073882]
16. Di Marco M, Ramassone A, Pagotto S, Anastasiadou E, Veronese A, Visone R. MicroRNAs in autoimmunity and hematological malignancies. Int J Mol Sci 2018;19:3139.
17. Lawrie CH, Gal S, Dunlop HM, Pushkaran B, Liggins AP, Pulford K, et al. Detection of elevated levels of tumour-associated microRNAs in serum of patients with diffuse large B-cell lymphoma. Br J Haematol 2008;141:672–5. [PubMed: 18318758]
18. Due H, Svendsen P, Bodker JS, Schmitz A, Bogsted M, Johnsen HE, et al. miR-155 as a biomarker in B-cell malignancies. Biomed Res Int 2016;2016:9513037. [PubMed: 27294145]
19. Sole C, Arnaiz E, Lawrie CH. MicroRNAs as biomarkers of B-cell lymphoma. Biomark Insights 2018;13:1177271918806840. [PubMed: 30349178]
20. Tam W Identification and characterization of human BIC, a gene on chromosome 21 that encodes a noncoding RNA. Gene 2001;274:157–67. [PubMed: 11675008]
21. Lawrie CH, Soneji S, Marafioti T, Cooper CD, Palazzo S, Paterson JC, et al. MicroRNA expression distinguishes between germinal center B cell-like and activated B cell-like subtypes of diffuse large B cell lymphoma. Int J Cancer 2007; 121:1156–61. [PubMed: 17487835]

22. Eis PS, Tam W, Sun L, Chadburn A, Li Z, Gomez MF, et al. Accumulation of miR-155 and BIC RNA in human B cell lymphomas. Proc Natl Acad Sci U S A 2005; 102:3627–32. [PubMed: 15738415]

23. Costinean S, Zanesi N, Pekarsky Y, Tili E, Volinia S, Heerema N, et al. Pre-B cell proliferation and lymphoblastic leukemia/high-grade lymphoma in E(mu)-miR155 transgenic mice. Proc Natl Acad Sci U S A 2006;103:7024–9. [PubMed: 16641092]

24. Babar IA, Cheng CJ, Booth CJ, Liang X, Weidhaas JB, Saltzman WM, et al. Nanoparticle-based therapy in an in vivo microRNA-155 (miR-155)-dependent mouse model of lymphoma. Proc Natl Acad Sci U S A 2012;109:E1695–704. [PubMed: 22685206]

25. Cheng CJ, Bahal R, Babar IA, Pincus Z, Barrera F, Liu C, et al. MicroRNA silencing for cancer therapy targeted to the tumour microenvironment. Nature 2015;518:107–10. [PubMed: 25409146]

26. Seto AG, Beatty X, Lynch JM, Hermreck M, Tetzlaff M, Duvic M, et al. Cobomarsen, an oligonucleotide inhibitor of miR-155, co-ordinately regulates multiple survival pathways to reduce cellular proliferation and survival in cutaneous T-cell lymphoma. Br J Haematol 2018;183:428–44. [PubMed: 30125933]

27. Ramachandiran S, Adon A, Guo X, Wang Y, Wang H, Chen Z, et al. Chromosome instability in diffuse large B cell lymphomas is suppressed by activation of the noncanonical NF-kappaB pathway. Int J Cancer 2015;136:2341–51. [PubMed: 25359525]

28. Cirone M, Conte V, Farina A, Valia S, Trivedi P, Granato M, et al. HHV-8 reduces dendritic cell migration through down-regulation of cell-surface CCR6 and CCR7 and cytoskeleton reorganization. Virol J 2012;9:92. [PubMed: 22583958]

29. Huskova H, Korecka K, Karban J, Vargova J, Vargova K, Dusilkova N, et al. Oncogenic microRNA-155 and its target PU.1: an integrative gene expression study in six of the most prevalent lymphomas. Int J Hematol 2015;102:441–50. [PubMed: 26261072]

30. Lim EL, Trinh DL, Scott DW, Chu A, Krzywinski M, Zhao Y, et al. Comprehensive miRNA sequence analysis reveals survival differences in diffuse large B-cell lymphoma patients. Genome Biol 2015;16:18. [PubMed: 25723320]

31. Musilova K, Mraz M. MicroRNAs in B-cell lymphomas: how a complex biology gets more complex. Leukemia 2015;29:1004–17. [PubMed: 25541152]

32. Mazan-Mamczarz K, Gartenhaus RB. Role of microRNA deregulation in the pathogenesis of diffuse large B-cell lymphoma (DLBCL). Leuk Res 2013;37: 1420–8. [PubMed: 24054860]

33. Zhu FQ, Zeng L, Tang N, Tang YP, Zhou BP, Li FF, et al. MicroRNA-155 downregulation promotes cell cycle arrest and apoptosis in diffuse large B-cell lymphoma. Oncol Res 2016;24:415–27. [PubMed: 28281962]

34. Zhang Y, Roccaro AM, Rombaoa C, Flores L, Obad S, Fernandes SM, et al. LNA-mediated anti-miR-155 silencing in low-grade B-cell lymphomas. Blood 2012; 120:1678–86. [PubMed: 22797699]

35. Tili E, Michaille JJ, Wernicke D, Alder H, Costinean S, Volinia S, et al. Mutator activity induced by microRNA-155 (miR-155) links inflammation and cancer. Proc Natl Acad Sci U S A 2011;108:4908–13. [PubMed: 21383199]

36. Riepsaame J, van Oudenaren A, den Broeder BJ, van Ijcken WF, Pothof J, Leenen PJ. MicroRNA-mediated down-regulation of M-CSF receptor contributes to maturation of mouse monocyte-derived dendritic cells. Front Immunol 2013;4:353. [PubMed: 24198819]

37. Caramuta S, Lee L, Ozata DM, Akcakaya P, Georgii-Hemming P, Xie H, et al. Role of microRNAs and microRNA machinery in the pathogenesis of diffuse large B-cell lymphoma. Blood Cancer J 2013;3:e152. [PubMed: 24121164]

38. Kaczmarek JC, Kowalski PS, Anderson DG. Advances in the delivery of RNA therapeutics: from concept to clinical reality. Genome Med 2017;9:60. [PubMed: 28655327]

39. Yin W, Rogge M. Targeting RNA: a transformative therapeutic strategy. Clin Transl Sci 2019;12:98–112. [PubMed: 30706991]

40. Gilles ME, Hao L, Huang L, Rupaimoole R, Lopez-Casas PP, Pulver E, et al. Personalized RNA medicine for pancreatic cancer. Clin Cancer Res 2018;24: 1734–47. [PubMed: 29330203]

41. Malik S, Bahal R. Investigation of PLGA nanoparticles in conjunction with nuclear localization sequence for enhanced delivery of antimiR phosphorothioates in cancer cells *in vitro*. J Nanobiotechnology 2019;17:57. [PubMed: 31010426]
42. Rupaimoole R, Slack FJ. MicroRNA therapeutics: towards a new era for the management of cancer and other diseases. Nat Rev Drug Discov 2017;16: 203–22. [PubMed: 28209991]
43. Jiang S, Zhang HW, Lu MH, He XH, Li Y, Gu H, et al. MicroRNA-155 functions as an OncomiR in breast cancer by targeting the suppressor of cytokine signaling 1 gene. Cancer Res 2010;70:3119–27. [PubMed: 20354188]
44. Ramdzan ZM, Nepveu A. CUX1, a haploinsufficient tumour suppressor gene overexpressed in advanced cancers. Nat Rev Cancer 2014;14:673–82. [PubMed: 25190083]
45. Matheson CJ, Backos DS, Reigan P. Targeting WEE1 kinase in cancer. Trends Pharmacol Sci 2016;37:872–81. [PubMed: 27427153]
46. Anastasiadou E, Boccellato F, Vincenti S, Rosato P, Bozzoni I, Frati L, et al. Epstein-Barr virus encoded LMP1 downregulates TCL1 oncogene through miR-29b. Oncogene 2010;29:1316–28. [PubMed: 19966860]
47. Anastasiadou E, Garg N, Bigi R, Yadav S, Campese AF, Lapenta C, et al. Epstein-Barr virus infection induces miR-21 in terminally differentiated malignant B cells. Int J Cancer 2015;137:1491–7. [PubMed: 25704079]
48. Anastasiadou E, Stroopinsky D, Alimperti S, Jiao AL, Pyzer AR, Cippitelli C, et al. Epstein-Barr virus-encoded EBNA2 alters immune checkpoint PD-L1 expression by downregulating miR-34a in B-cell lymphomas. Leukemia 2019;33:132–47. [PubMed: 29946193]
49. Di Napoli A, Al-Jadiri MF, Talerico C, Duranti E, Pilozzi E, Trivedi P, et al. Epstein-Barr virus (EBV) positive classical Hodgkin lymphoma of Iraqi children: an immunophenotypic and molecular characterization of Hodgkin/Reed-Sternberg cells. Pediatr Blood Cancer 2013;60:2068–72. [PubMed: 24000236]
50. Rosato P, Anastasiadou E, Garg N, Lenze D, Boccellato F, Vincenti S, et al. Differential regulation of miR-21 and miR-146a by Epstein-Barr virus-encoded EBNA2. Leukemia 2012;26:2343–52. [PubMed: 22614176]
51. Trivedi P, Slack FJ, Anastasiadou E. Epstein-Barr virus: from kisses to cancer, an ingenious immune evader. Oncotarget 2018;9:36411–2. [PubMed: 30559926]
52. Gottwein E, Mukherjee N, Sachse C, Frenzel C, Majoros WH, Chi JT, et al. A viral microRNA functions as an orthologue of cellular miR-155. Nature 2007;450: 1096–9. [PubMed: 18075594]
53. Zhao Y, Xu H, Yao Y, Smith LP, Kgosana L, Green J, et al. Critical role of the virus-encoded microRNA-155 ortholog in the induction of Marek's disease lymphomas. PLoS Pathog 2011;7:e1001305. [PubMed: 21383974]

Translational Relevance

Our *in vitro* and *in vivo* preclinical studies recapitulate the important role of miR-155 in the pathogenesis of diffuse large B-cell lymphoma (DLBCL) and in particular of the most aggressive and hard-to-treat non–germinal center B-cell subtype DLBCL, also called activated B-cell subtype of DLBCL (non-GCB/ABC-DLBCL). Cobomarsen, an anti–miR-155 compound, effectively inhibited proliferation and induced apoptosis in ABC-DLBCL cell lines with high endogenous miR-155 expression and reduced tumor growth in xenografts. Most importantly, administration of this compound in a patient with DLBCL who was resistant to all previous therapeutic regimens provided new insights for the safety and therapeutic potential of cobomarsen monotherapy for management of patients with refractory ABC-DLBCL. Cobomarsen-based therapy could be extended not only to ABC-DLBCLs but also to other types of lymphomas characterized by high miR-155 expression, either as a single agent or in combination with other therapeutic regimens.

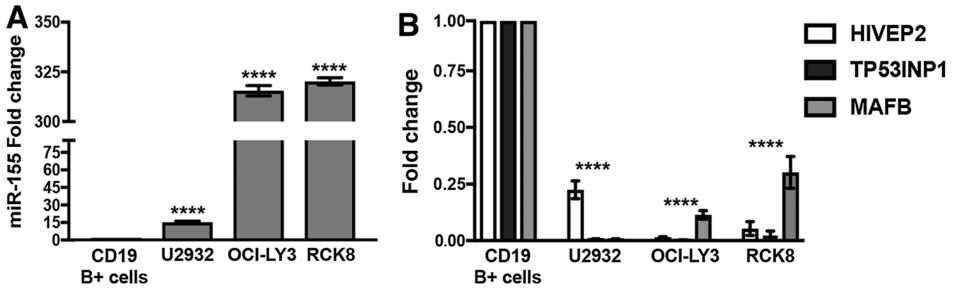

Figure 1.:

High expression of miR-155 in DLBCL cell lines and correlation with target gene expression. **A,** The fold change of miR-155 expression in three ABC-type DLBCL cell lines was assessed by qRT-PCR. MiR-155 fold change was compared with CD19 B+ isolated from healthy donors and normalized to RNU6 housekeeping gene. Statistical analysis was performed with unpaired, two-tailed *t* test: ****, $P < 0.0001$. Fold change represents the average (±SD) of three independent experiments, each performed in technical triplicates. **B,** The fold change of miR-155 target genes, HIVEP2, TP53INP1, and MAFB expression was assessed by qRT-PCR: The fold change expression of each target gene in each cell line was compared with the one of CD19 B+ cells and was normalized to GAPDH. Unpaired, two-tailed *t* test was applied: ****, $P < 0.0001$. Fold change represents the average (±SD) of three independent experiments, each performed in technical triplicates.

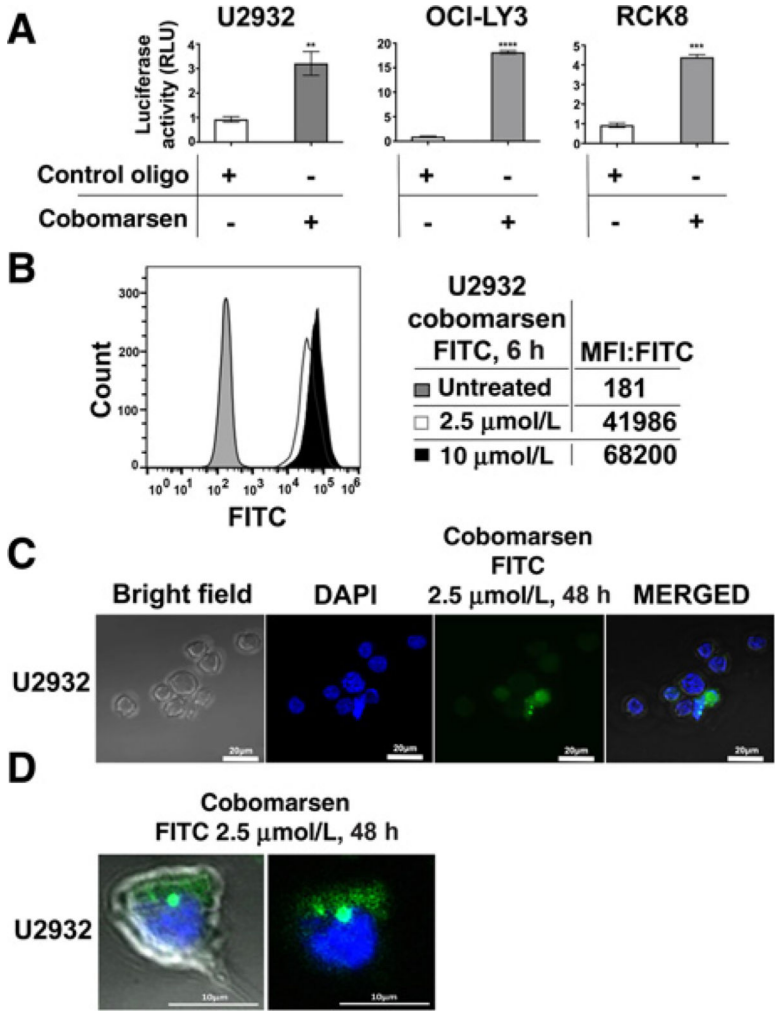

Figure 2.:

Unassisted delivery of cobomarsen in ABC-DLBCL cell lines. **A,** Reduction in endogenous miR-155 activity by cobomarsen: Luciferase activity was measured 24 hours after treatment with cobomarsen or control oligonucleotide. Each treatment was performed in triplicates, and the experiment was repeated three times. Relative luminescence units (RLU) indicate the ratio of Renilla luciferase (hRluc) expression normalized against firefly luciferase (fluc), (hRluc/fluc), of the miR-155 biosensor. The control oligo– and cobomarsen-treated cell lines were compared. Unpaired, two-tailed *t* test was applied as a mean value for each experiment repeated three times and in triplicates. The calculated *P* values between control oligo–treated versus cobomarsen-treated cell line are: U2932: **, $P < 0.01$; OCI-LY3: ****, $P < 0.0001$; RCK8: ***, $P < 0.001$. **B,** Cobomarsen uptake in recipient lymphoma cells: Two different concentrations (2.5 µmol/L, 10 µmol/L) of FITC-conjugated cobomarsen were directly added in the culture of U2932 cell line. Histograms show the MFI at both concentrations compared with the cobomarsen untreated cells, at 6 hours postdelivery. MFI was measured by flow cytometer, and the data were analyzed by Kaluza for Gallios Software. **C** and **D,** Subcellular localization of cobomarsen: **C,** Confocal microscopy images of 2.5 µmol/L FITCH-conjugated cobomarsen in U2932 cell line at 48 hours postdelivery. **D,** A higher

magnification (20×) demonstrates cobomarsen as green fluorescent dot next to the nucleus, blue colored, with 4′,6-diamidino-2-phenylindole (DAPI). Confocal images were acquired using 20× and 10× objectives with the Zeiss LSM 880 confocal microscope.

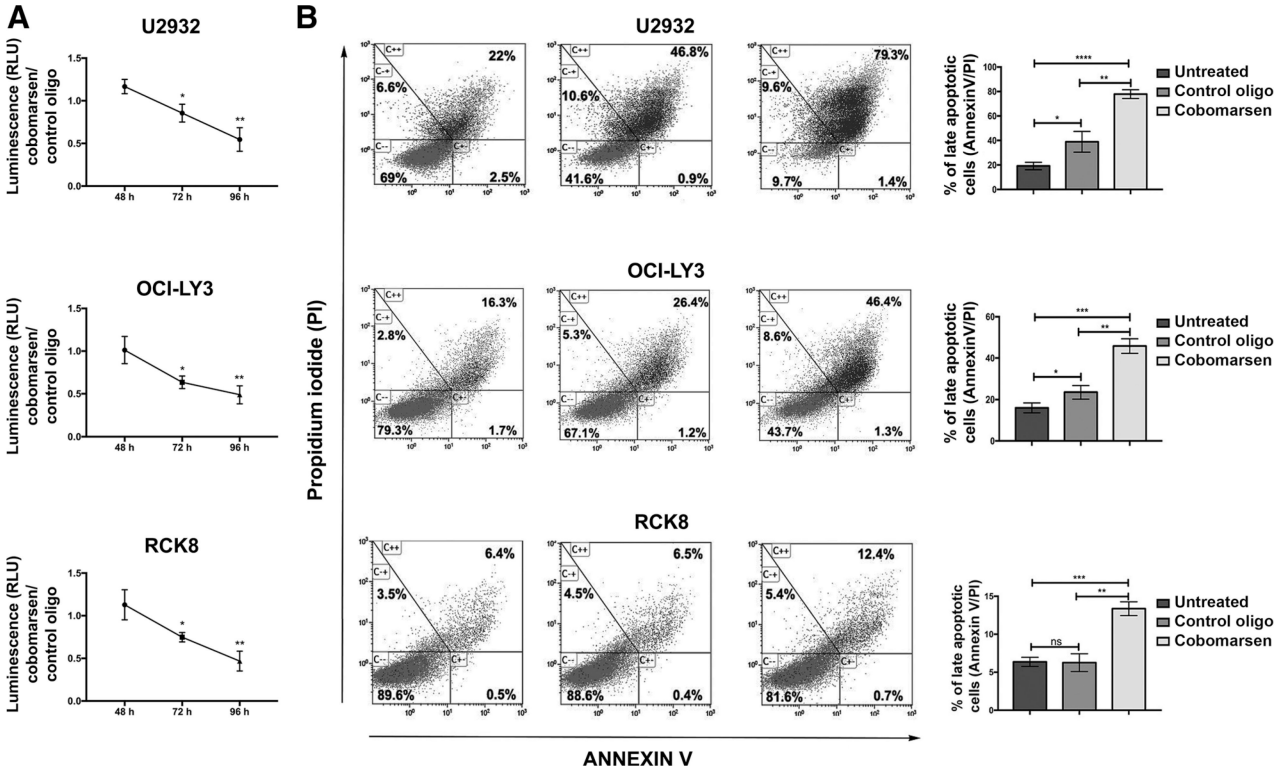

Figure 3.:

Proliferation and apoptosis in DLBCL cell lines upon cobomarsen treatment. **A,** The proliferation graphs indicate luminescence (RLU) measurements as a ratio of cobomarsen/ control oligonucleotide RLU at 48, 72, and 96 hours postdelivery of 10 μmol/L cobomarsen or 10 μmol/L control oligonucleotide. The experiment was performed three times and in triplicates. Unpaired, two-tailed *t* test was applied to calculate the statistical significance of the difference between the average of RLU ratio measurements at 72 and 96 hours compared with corresponding average of RLU at 48 hours. *, $P < 0.05$; **, $P < 0.01$. **B,** Annexin V/PI measurement of late apoptotic cells (double stained for Annexin V and PI) 96 hours following treatment with 10 μmol/L cobomarsen. For each cell line, the % of late apoptotic cells upon treatment was compared with the % of untreated cells, by setting the same threshold. One out of three representative experiments is shown. The histograms for each cell line, at the right side of the figure, show the mean values from three independent apoptosis assays, comparing the % of untreated, control oligonucleotide– and cobomarsen-treated cells. U2932: *, $P < 0.05$; **, $P < 0.01$; ****, $P < 0.0001$. OCY-LY3: *, $P < 0.05$; **, $P < 0.01$; ***, $P < 0.001$. RCK8: **, $P < 0.01$; ***, $P < 0.001$. Statistical analysis was performed with unpaired, two-tailed *t* test. Kaluza for Gallios Software was used for analysis.

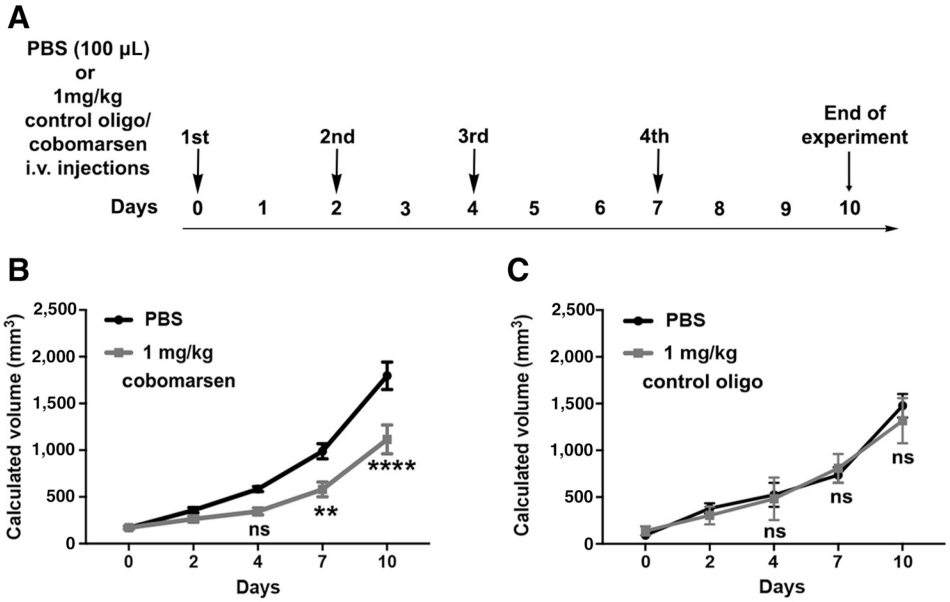

Figure 4.:

Effect of cobomarsen on tumor growth *in vivo*. **A,** Timeline of *in vivo* inoculations of cobomarsen and control oligonucleotide: The tumors began to grow 9–12 days after injection. Mice were enrolled in the study when the tumor volume reached a range of 150–200 mm^3. Subsequently, 12 mice were injected intravenously with 100 µL PBS and 12mice with 1 mg/kg cobomarsen. In parallel, 3mice were injected with 100 µL PBS and 3 mice with 1 mg/kg of a control oligonucleotide on days 0, 2, 4, and 7 after enrollment. Seventy-two hours after the last dose, mice were euthanized. All tumor volume measurements were taken before the injections. **B,** Tumor growth: The mean value of the calculated volumes (mm^3) of the xenografts at the indicated time points, in 12 mice treated with 1 mg/kg cobomarsen in comparison with the mean of the calculated volumes in 12 mice treated with 100 µL PBS, show a significant reduction in time, at the 7th day and at the 10th day, of 12 mice. **, $P < 0.01$; ****, $P < 0.0001$. **C,** Tumor growth: The mean value of the calculated volumes (mm^3) of the xenografts and in the indicated time points shows no difference between the groups of 3mice treated with 100 µL PBS compared with the group of 3mice treated with 1 mg/mL control oligo. The statistical significance of the mean value of the tumor volumes in different time points between the groups of mice was performed using two-way ANOVA with Sidak multiple comparisons test.

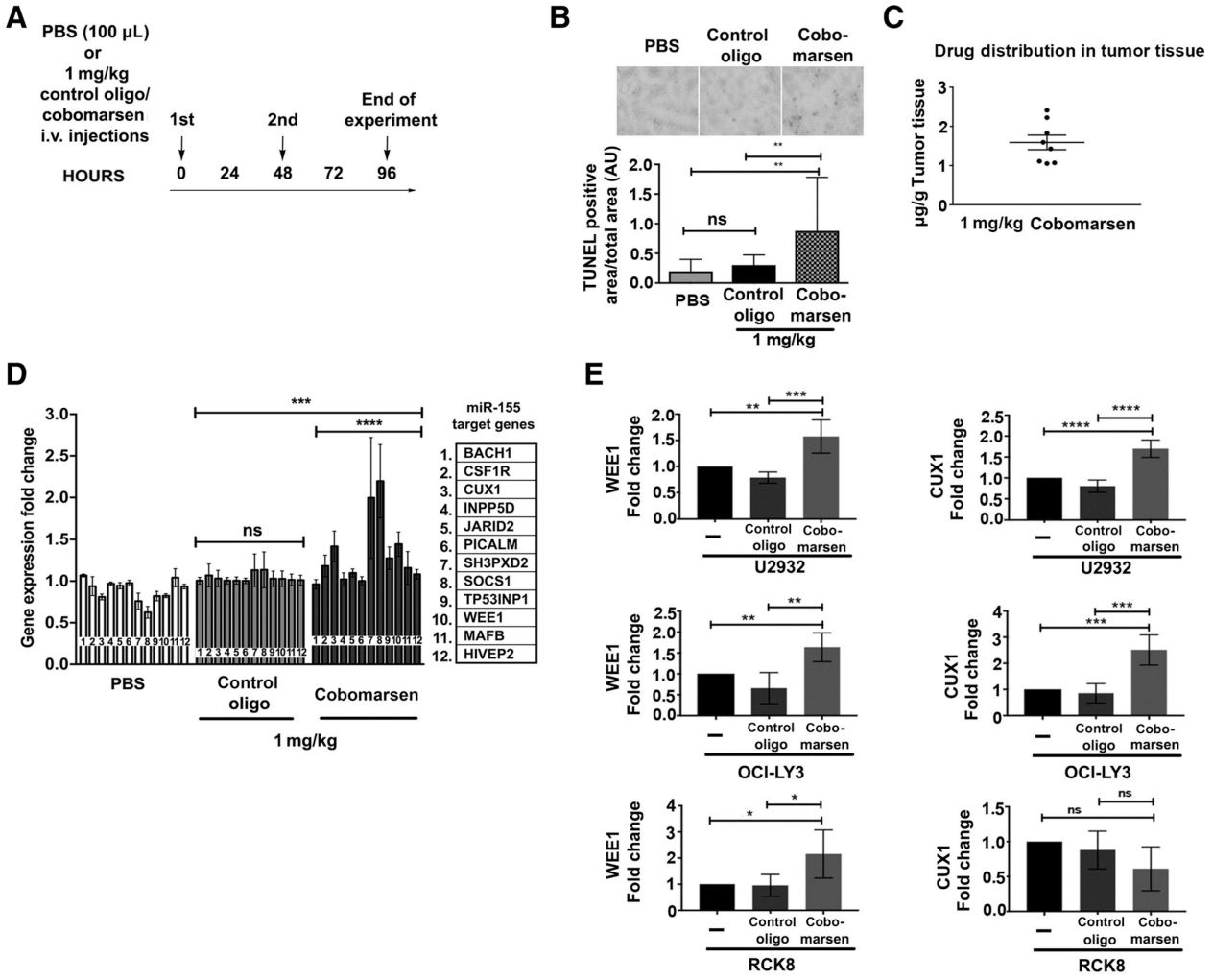

Figure 5.:

Cobomarsen derepresses miR-155 target gene expression *in vivo* and *in vitro.* **A,** Timeline of cobomarsen-treated xenografts used to assess pharmacodynamic effects: Mice were randomly enrolled into groups when tumors reached a volume of 150–200mm^3 ($N = 8$ for each of three groups; PBS, control oligonucleotide, and cobomarsen). Mice were injected intravenously with either PBS, 1 mg/kg control oligonucleotide, or 1 mg/kg cobomarsen at 0 and 48 hours after enrollment. Twenty-four hours after the last dose, mice were sacrificed and tumor tissue was harvested. **B,** Cobomarsen induces tumor apoptosis: Detection of apoptotic cells in mice tumor tissues 24 hours following the final dose of PBS, control oligonucleotide, or cobomarsen. Three representative photos of mouse tumor tissue cryosections processed with the TUNEL chromogenic apoptotic assay. Chromogen 3,3′-diaminobenzidine staining reveals the brown spots that indicate apoptotic cells. The analysis was performed for a total of 4–10 fields per tumor. The results are reported as arbitrary unit (AU) and represent an average value from 3 mice per treatment (PBS, 1 mg/kg-control oligonucleotide, 1 mg/kg cobomarsen). Statistical analysis was performed with unpaired, two-tailed *t* test. **, $P < 0.01$ for cobomarsen versus PBS, and for cobomarsen versus control oligo. **C,** Drug distribution in tumor tissue: Quantification of cobomarsen in the

tumors from treated mice ($n = 8$), represented by black dots, using S1 nuclease protection assay. **D,** qRT-PCR analysis ofmiR-155 target gene expression in cobomarsen-treated xenografts: Mice were euthanized, and tumors were harvested 24 hours after the last injection with either PBS, control oligonucleotide, or cobomarsen. RNA was extracted from tumors, and the expression of direct miR-155 target genes was evaluated by qRT-PCR. Two-way ANOVA, Tukey multiple comparison test, between the mean values of miR-155 target gene expression per treatment from group of mice treated with PBS versus oligonucleotide control treated, ****, $P < 0.0001$ and between the group of mice treated with oligonucleotide versus cobomarsen treated ***, $P < 0.001$. $N = 8$ mice per group. **E,** miR-155 target genes are derepressed in cobomarsen-treated DLBCL cell lines: qRT-PCR analysis of miR-155 target genes CUX1 and WEE1 upon treatment with 10 μmol/L cobomarsen, at 96 hours in U2932, OCI-LY3, and RCK8 DLBCLs. For U2932 CUX1: ****, $P < 0.0001$ andWEE1 ***, $P < 0.001$; **, $P < 0.01$. For OCI-LY3 CUX1: ***, $P < 0.001$ and WEE1: **, $P < 0.01$. For RCK8 CUX1, n.s.: $P = 0.1851$ and WEE1: *, $P < 0.05$. P values were calculated with unpaired, two-tailed t test. The experiment was performed in triplicates and repeated at least two times.

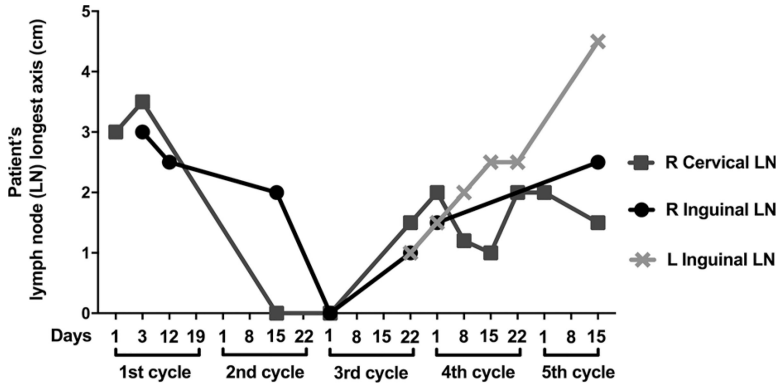

Figure 6.:

Patient's lymph node (LN) measurements over time, during the cobomarsen treatment. The longest axis of right (R) cervical LN, R inguinal LN, and left (L) inguinal LN was measured with a ruler after palpable medical examinations of the tumor mass. The size of the tumor mass in centimeters was assessed at the indicated days for each of the five cycles. Cobomarsen i.v. injections (600 mg/injection) were performed at the same day as the physical exams and measurements (1st cycle: 6 injections; 2nd, 3rd, and 4th cycle: 4 injections/cycle; and 5th cycle: 3 injections). LN, measurements were performed during physical examination, at the days indicated in the graph: for R cervical LN, the measurements were started at cycle 1, day 1, while for R inguinal LN, measurements were started at cycle 1, day 3. L inguinal LN was noted during cycle 3 on the 22nd day.

Table 1.

Tumor xenograft growth study.

Group[a]	Number of mice/group	Dose	Miragen compounds	Route of administration	Schedule[b]
A	12	100 μL	PBS	i.v.	day 0, 2, 4, and 7 following enrollment into group
B	12	1 mg/kg	Cobomarsen	i.v.	day 0, 2, 4, and 7 following enrollment into group
C	3	100 μL	PBS	i.v.	day 0, 2, 4, and 7 following enrollment into group
D	3	1 mg/kg	Control oligonucleotide	i.v.	day 0, 2, 4, and 7 following enrollment into group

[a] Five- to six-week-old female NSG (*NOD*.Cg-Prkdc^{scid} Il2rg^{tm1Wjl}/SzJ, strain number 005557) mice were divided in four groups: A and B contained 12 mice each that were injected intravenously, in the tail vein, with 100 μL of the vehicle PBS or with 1 mg/kg cobomarsen, respectively. Group A served as control for group B. The C and D groups contained 3 mice each, injected intravenously either with 100 μL PBS alone or 100 μL PBS containing 1 mg/kg of the control oligonucleotide, respectively. Group C served as control for group D.

[b] For the tumor growth study, the time points of intravenous injections were scheduled as described in the table.

Table 2.

Pharmacodynamic study.

Group[a]	Number of mice/group	Dose	Miragen compounds	Route of administration	Schedule[b]
1	8	100 μL	PBS	i.v.	Injection at 0 and 48 hours after enrollment
2	8	1 mg/kg	Control oligonucleotide	i.v.	Injection at 0 and 48 hours after enrollment
3	8	1 mg/kg	Cobomarsen	i.v.	Injection at 0 and 48 hours after enrollment

[a]Five- to six-week-old female NSG (*NOD*.Cg-Prkdc^{scid} Il2rg^{tm1Wjl}/SzJ, strain number 005557) mice were divided in three groups: 1, 2, and 3 containing 8 mice each. All mice were injected intravenously in the tail vein with 100 μL of the vehicle PBS, the second with 100 μL of 1 mg/kg control oligonucleotide in PBS, and the third with 100 μL of 1 mg/kg of cobomarsen in PBS.

[b]For the pharmacodynamic study, all the injections were performed at the beginning of the study, indicated as 0 and at 48 hours after enrollment.